Acta Crystallographica Section D
Biological Crystallography
ISSN 0907-4449

Individual interactions influence the crystalline order for membrane proteins

A. Camara-Artigas,† C. L. Magee, J. C. Williams and J. P. Allen*

Department of Chemistry and Biochemistry, Arizona State University, Tempe, AZ 85287-1604, USA

† Permanent address: Dpto Química Física, Bioquímica y Química Inorgánica, Universidad de Almería, Spain.

Correspondence e-mail: jallen@asu.edu

Received 30 March 2001
Accepted 3 July 2001

PDB References: TL(*M*21) Thr→Leu, 1jgw; TD(*M*21) Thr→Asp, 1jgx; YF(*M*76) Thr→Phe, 1jgy; YK(*M*76) Thr→Lys, 1jgz; EL(*L*205) Glu→Leu, 1jh0.

The role of contact interactions in the crystallization of membrane proteins was assessed by mutation of amino-acid residues on the surface of the reaction center from *Rhodobacter sphaeroides*. Five single-site mutants were constructed, with changes in contact regions found in the trigonal and tetragonal forms but not the orthorhombic form. Crystallization trials for the tetragonal form yielded either no crystals or crystals with an altered morphology, whereas crystals grew in the other two forms, indicating that these interactions are essential for the stability of the tetragonal crystals. Changes in the structures determined by X-ray diffraction of trigonal crystals for each mutant were related to the quality of the diffraction. Significant differences in the resolution limit of the crystals were associated with the loss of specific interactions between neighboring proteins. The results suggest that the contact regions are crucial for obtaining highly ordered crystals of membrane proteins.

1. Introduction

Integral membrane proteins play critical roles in many cellular processes, but our understanding of their function remains limited owing to the challenges in obtaining crystals of these proteins that are suitable for X-ray diffraction studies (Bowie, 2000). Difficulties stem from the detergents needed to solubilize these proteins by binding to the region of the protein normally found in the membrane. This requirement both tremendously increases the number of crystallization conditions that must be screened and excludes a large region of the protein surface from the formation of protein–protein contacts that are necessary to stabilize the crystalline state. Membrane proteins such as the reaction center, the cytochrome bc_1 complex and cytochrome *c* oxidase contain large extramembranous segments on one or both sides of hydrophobic transmembrane α-helices; the contacts in crystals of these proteins are generally found in these hydrophilic regions (Deisenhofer *et al.*, 1985; Iwata *et al.*, 1995; Tsukihara *et al.*, 1996; Xia *et al.*, 1997; Zhang *et al.*, 1998). Packing in crystals of proteins that do not include any significant portion of the protein that extends from the membrane shows even more limited protein–protein contacts. For example, only one or two major interactions are found in crystals of the light-harvesting complex II from *Rhodopseudomonas acidophila* (McDermott *et al.*, 1995) and the KcsA ion channel (Doyle *et al.*, 1998). In several cases, significant contacts are provided by bridging molecules such as heptanetriol in the crystals of the light-harvesting complex II from *Rhodospirillum molischianum* (Koepke *et al.*, 1996) and a gold compound in crystals of the

MscL channel (Chang *et al.*, 1998). Specifically bound detergent molecules also have been found to play a critical role in establishing crystal contacts involving a hydrophobic region of fumarate reductase (Iverson *et al.*, 1999). Thus, a challenge for the crystallization of membrane proteins is that these few interactions provide a tenuous opportunity for the ordering of the proteins in crystals.

The role of surface residues in crystallization has been characterized for water-soluble proteins such as lysozyme (Matthews, 1995; Iyer *et al.*, 2000), but less is known about their significance in the crystallization of membrane proteins, where they are likely to be more prominent because these favorable interactions are restricted to regions external to the membrane. The contribution of contact regions in the crystallization of membrane proteins has been examined by addition of a hydrophilic domain, use of a protein isolated from several different species and manipulation of surface residues (Iwata *et al.*, 1995; Zhang *et al.*, 1998; Pautsch *et al.*, 1999); however, a general mechanism for optimizing these interactions has not been developed. In this work, we report on how alterations of the amino-acid residues at contact sites in the reaction center, a model membrane-protein system, influence the ability to crystallize the protein in several forms as well as the quality of the crystals as measured using X-ray diffraction. Since the reaction center packs differently for each of several space groups, the contact sites can be selectively altered and the effects on the crystallization of each form compared.

The reaction center serves as a useful model system for studying the crystallization of membrane proteins as the protein is stable in a variety of detergents, can be altered using molecular genetics and has been extensively characterized (Feher *et al.*, 1988). The reaction center from *Rhodobacter sphaeroides* can be crystallized in three different space groups yielding wild-type structures (Allen *et al.*, 1987; Chang *et al.*, 1991; Ermler *et al.*, 1994; Stowell *et al.*, 1997) with resolution limits of 2.8 Å for the orthorhombic form ($P2_12_12_1$), 2.65 Å for the trigonal form ($P3_121$) and 2.2 Å for the tetragonal form ($P4_32_12$). The residues from the three protein subunits, *L*, *M* and *H*, participating in the contact sites are found in different hydrophilic regions of the reaction center (Fig. 1*a*). Several regions are common to all three forms, but other regions of the protein participate in contact sites only in one or two of the forms. In general, the orthorhombic form, which diffracts the poorest of the three forms, has the fewest contact regions. The tetragonal form has a unique contact formed by Glu*L*205 and residues Tyr*M*76 and Lys*M*110 from a symmetry-related protein (Fig. 1*b*). Similarly, an interaction involving Thr*M*21, Tyr*L*73 and Lys*L*82 is found in the trigonal and tetragonal forms but not in the orthorhombic form.

To test the importance of the protein–protein interactions in establishing the crystal order, we targeted specific amino acids in the contact regions of particular forms. These mutants were constructed to determine if a single protein interaction would have an effect on the crystal order and were not necessarily designed to produce better quality crystals. In most of the mutants, an interaction such as a hydrogen bond is necessarily removed by the amino-acid change. Five single-site mutations were made. The changes Thr*M*21→Leu [TL(*M*21)] and Thr*M*21→Asp [TD(*M*21)] were designed to influence

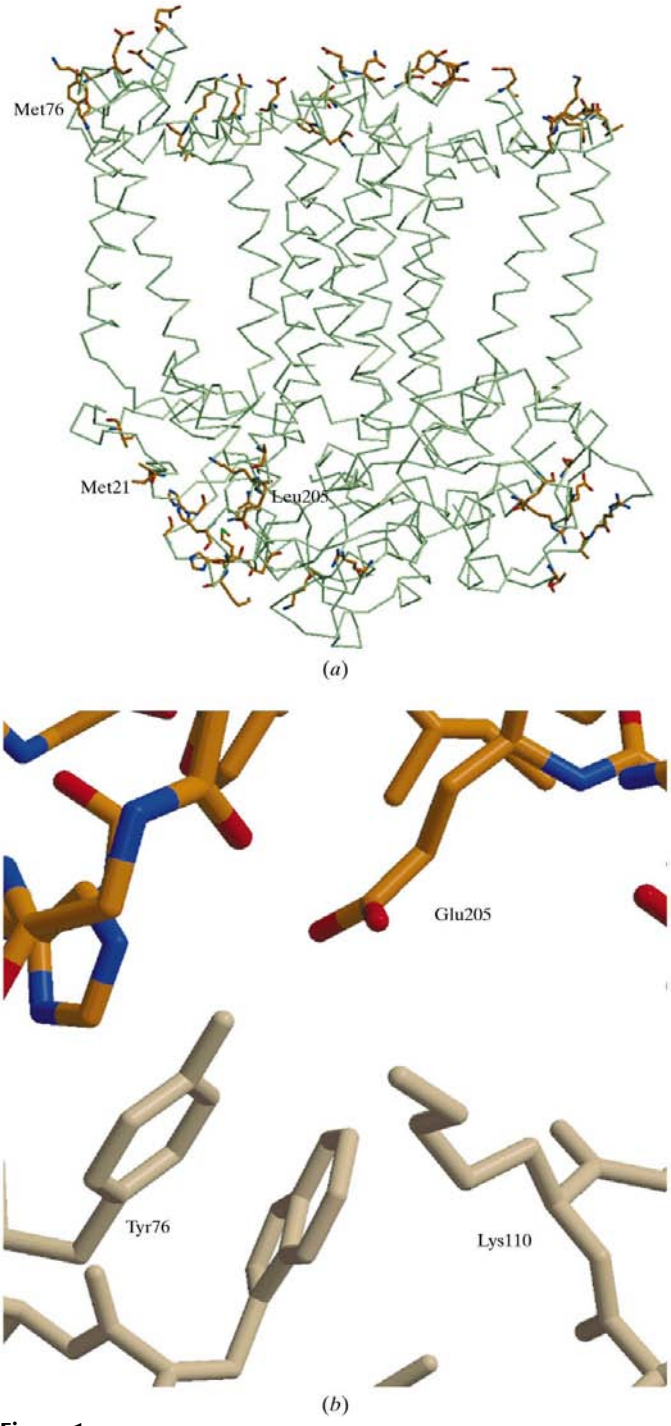

Figure 1
Structure of the wild-type reaction center from *R. sphaeroides*. (*a*) Backbone with the residues that have been found in a contact site in any one of the three crystal forms. All of the residues are located in the hydrophilic regions away from the central membrane-spanning region. The three residues at which mutations were made are labeled. (*b*) One of the contact interactions that is found only in the tetragonal form. Shown are residues Glu*L*205 of one protein (shaded with atom types colored) and Tyr*M*76 and Lys*M*110 of a neighboring protein (shaded light tan). The residues form a bridge and hydrogen bonds that probably contribute to the high degree of crystalline order of this form.

primarily both the trigonal and tetragonal forms, while the mutations Tyr*M*76→Phe [YF(*M*76)], Tyr*M*76→Lys [YK(*M*76)] and Glu*L*205→Leu [EL(*L*205)] were designed to act preferentially upon the tetragonal form.

2. Experimental

2.1. Mutagenesis, protein isolation and crystallization

Mutants of the reaction center were constructed and the proteins isolated as previously described (Williams *et al.*, 1992). Before crystallization, samples were further purified with a tertiary amine column using FPLC (Pharmacia LKB, Uppsala, Sweden). After this chromatography step, the protein was used either directly for the crystallization solutions or dialyzed against either 15 m*M* Tris–HCl pH 8, 0.025% LDAO, 1 m*M* EDTA or 15 m*M* Tris–HCl pH 8.0, 0.8% β-octyl glucoside, 1 m*M* EDTA. Preparations and crystallization trials for the wild-type reaction center were performed in parallel with the mutants.

Crystallization trials were performed for the reaction centers from the wild type and each mutant in the orthorhombic, trigonal and tetragonal forms (Allen *et al.*, 1987; Ermler *et al.*, 1994; Allen, 1994). For all three cases, drops containing 20–50 µl of a protein solution were equilibrated by vapor diffusion against a 1 ml reservoir. For the orthorhombic form, the protein solution contained reaction centers at a concentration of 10 mg ml^{-1}, 0.06% LDAO, 12% polyethylene glycol 4000, 0.3 *M* NaCl, 3.9% heptanetriol and 15 m*M* Tris–HCl pH 8.0. The reservoir contained 22% polyethylene glycol 4000, 0.6 *M* NaCl and 15 m*M* Tris–HCl pH 8.0. For the trigonal form, the protein solution contained 20 mg ml^{-1} protein, 0.08% LDAO, 0.75 *M* potassium phosphate pH 7.5, 3.5% heptanetriol and the reservoir contained 1.6 *M* potassium phosphate pH 7.5. For the tetragonal form, the protein solution contained 16 mg ml^{-1} protein, 5.0% polyethylene glycol 4000, 0.85% β-octyl glucoside, 0.4% benzamidine hydrochloride and the reservoir contained 32% polyethylene glycol 4000. In addition to tests with these specific conditions, crystallization trials were performed in each case with small variations of approximately 10% in the concentrations of the detergents and amphiphiles and larger (∼30%) variations in the salt and protein concentrations. For every set of conditions, 5–10 identical wells were prepared.

2.2. Measurement of X-ray diffraction data

For the wild type and each mutant, data were initially measured using a rotating-anode X-ray generator with an R-AXIS II detector (Rigaku, The Woodlands, Texas) and processed using *DENZO* (Otwinowski & Minor, 1997). To measure the diffraction data at the maximum possible resolution, data sets were subsequently measured at the Stanford Synchrotron Radiation Laboratory (beamline 7-1) and processed using *MOSFLM* (Leslie, 1999). For the wild type and each mutant, the data sets were collected from crystals in the trigonal form mounted in capillaries at room temperature. Low-temperature measurements were avoided because of the possible introduction of disorder arising from freezing. Data sets obtained from one crystal were used for most mutants, except that two data sets were merged for TL(*M*21). Three mutants exhibited an apparent increase in sensitivity to X-rays: TL(*M*21), YF(*M*76) and YK(*M*76). As a result of this sensitivity, the use of single data sets for YF(*M*76) and YK(*M*76) resulted in a low level of completeness. The incompleteness of the most X-ray sensitive mutant TL(*M*21) was overcome by merging three data sets, but the resulting $R_{\rm merge}$ was high. The highest quality data sets are from the synchrotron data, except for EL(*L*205), which exhibited an unusually large variation in diffraction quality, with the best data set being measured using the R-AXIS system. For each mutant, diffraction data were measured from between two and four crystals and were processed independently.

2.3. Structure determination

The three-dimensional structure was determined for the wild type and each of the single-site mutants using X-ray data measured for the trigonal crystals. The starting model was the reaction center solved in the trigonal form (McAuley *et al.*, 1999; PDB file 1qov) with the appropriate amino-acid substitutions at the mutated sites. Each model was refined using

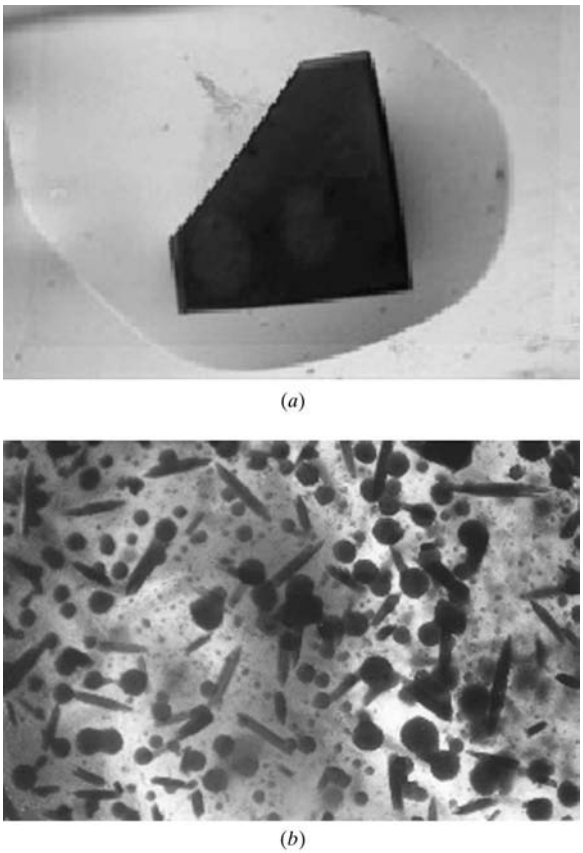

Figure 2
Crystals, grown under identical conditions, of reaction centers from (*a*) wild type and (*b*) the mutant EL(*L*205). The wild-type crystals shown in (*a*) belong to the tetragonal space group $P4_32_12$ (Table 1). The mutant shows a clearly different morphology to that observed for wild-type reaction centers and a significant decrease in size. The scales are the same, with the wild-type crystal having a length of 10 mm.

Table 1
Crystallization summary for the wild type and mutants.

	Observation of crystals† for different strains‡					
	Wild type	TL(*M*21) Thr→Leu	TD(*M*21) Thr→Asp	YF(*M*76) Tyr→Phe	YK(*M*76) Tyr→Lys	EL(*L*205) Glu→Leu
Orthorhombic $P2_12_12_1$	+	+	+	+	−§	+
Trigonal¶ $P3_121$	+	+	+	+	+	+
Tetragonal $P4_32_12$	+	−	−	−	New form††	New form††

† Sizes of the crystals varied, with the largest crystals typically having dimensions of 1 × 1 × 10 mm for orthorhombic, 3 × 3 × 10 mm for trigonal 10 × 10 × 2 mm for tetragonal. ‡ Subunit and residue number shown in parentheses of strain name; the mutation is listed on the second line. § The lack of crystals for YK(*M*76) may be spurious. ¶ All of these crystals yielded diffraction data as summarized in Table 2. †† These crystallization conditions yielded a new crystal form as shown in Fig. 2(*b*). Typical tetragonal crystals for the wild type are shown in Fig. 2(*a*).

rigid-body refinement followed by least-squares refinement and molecular dynamics using *CNS* (Brünger & Rice, 1997) and modeled using *O* (Jones *et al.*, 1991). The mutant structures were refined without the presence of the water molecules and ions at the contact sites. The refinement statistics and the quality of the models were evaluated using *PROCHECK* (Laskowski *et al.*, 1993). Figures were produced using *Raster3D* (Merritt & Bacon, 1997) and *XTALVIEW* (McRee, 1993). Evident in the electron density for the wild-type structure were features not previously identified, which will be described elsewhere.

3. Results

3.1. Effect of mutations on crystallization

For each mutant and the wild type, crystallization experiments were set up using individual conditions that result in the three crystal forms for the wild type (Table 1). Between five and ten identical wells were prepared with each of the three crystallization solutions and these trials were repeated using two or three different preparations of the protein. Crystals were obtained in the orthorhombic form for all mutants except for YK(*M*76). These crystals had a similar morphology and diffraction quality as the wild type, but because of the limited quality of this form further characterization of these crystals was not pursued and the lack of crystals for YK(*M*76) may be spurious. We conclude that to a first approximation the orthorhombic form was not strongly affected by the mutations, consistent with the design that these changes are not in contact regions for this form.

For the trigonal form, crystals were obtained for each mutant with the same morphology as wild type. Crystals of one mutant, TL(*M*21), only appeared after two months compared with two to three weeks for the wild type and the other mutants. In contrast, only two mutants, YK(*M*76) and EL(*L*205), yielded crystals using the tetragonal conditions. These crystals were small and had a different morphology to the wild type (Fig. 2). The mutations clearly had a drastic effect on the ability to obtain the tetragonal form, consistent with the location of these residues in a contact region for this form. These results show that a single amino-acid residue in a unique contact region can govern the disposition of a crystallization trial.

3.2. Structural changes associated with crystalline order

To relate the diffraction quality to specific structural changes, full data sets were measured for crystals of each of the mutants in the trigonal form and the three-dimensional structures were solved. Representative sets are presented in Table 2 and only those features found in every data set are described. The diffraction data for the TL(*M*21), YF(*M*76) and YK(*M*76) mutants have a quality comparable to wild type, while the data from crystals of the TD(*M*21) and EL(*L*205) mutants were consistently of poorer quality. The three-dimensional structures showed that the only significant alterations were near the mutation sites, with minimal backbone changes compared with the wild-type structure, indicating that the lower diffraction quality was a consequence of specific changes at the contact sites.

Examination of the contact region near Thr*M*21 showed a region containing several water molecules that provides an interacting bridge between the symmetry-related proteins in the wild type through a hydrogen-bond network (Fig. 3). The mutation of Thr to Leu at *M*21 results in

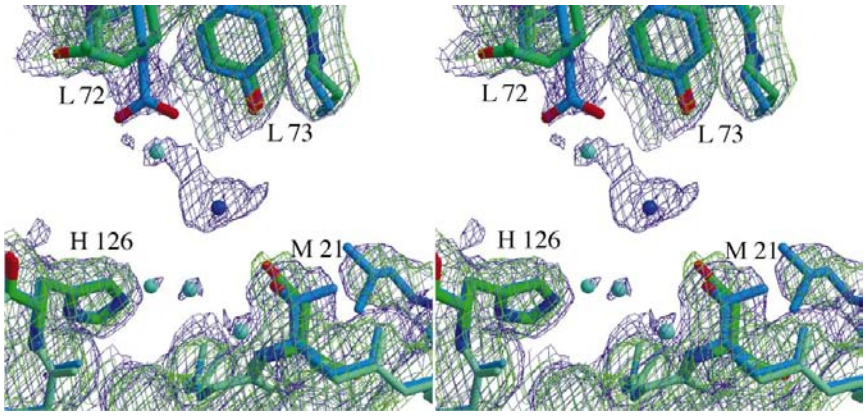

Figure 3
Stereo diagram of a contact region for the trigonal form in the wild type (blue shade) and the TD(*M*21) mutant (green shade). In the wild type, residue Thr*M*21 of one protein forms a contact with residue Tyr*L*73 of the neighboring protein through a bridging molecule that is tentatively identified as an ion (dark sphere). Also involved in these contact interactions are His*H*126 near *M*21, Glu*L*72 and Lys*L*82 (not shown) of the symmetry-related protein and several water molecules (light spheres). Replacement of Thr by Asp in the TD(*M*21) mutant results in loss of all electron density associated with the bridging ion and water molecules, resulting in no close contacts between the two proteins. The electron-density maps are contoured at 1σ and calculated at the highest resolution possible in each case; calculation of each map at 3.0 Å resolution does not alter the features discussed.

Table 2
Diffraction and structural data for the wild type and mutants.

Values in parentheses are for the last 0.1 Å shell.

	Strain†					
	Wild type	TL(*M*21) Thr→Leu	TD(*M*21) Thr→Asp	YF(*M*76) Tyr→Phe	YK(*M*76) Tyr→Lys	EL(*L*205) Glu→Leu
Unit-cell parameters‡ (Å)						
a, *b*	141.8	142.6	142.1	141.7	142.6	141.8
c	187.5	187.4	187.7	186.8	187.6	187.4
Resolution limit§ (Å)	2.55	2.8	3.0	2.7	2.7	3.5
Total reflections	157490	155581	128588	75641	177373	114799
Unique reflections	68536	51118	39407	35679	42176	26839
F/σ	37.0 (3.1)	20.2 (2.9)	21.0 (2.3)	18.0 (2.1)	25.2 (2.4)	21.0 (1.7)
R_{merge} (%)	14.7 (18.2)	25.4 (35.8)	14.3 (26.6)	10.3 (21.0)	16.6 (32.5)	23.2 (28.1)
Completeness (%)	95.9 (85.4)	93.5 (87.2)	88.8 (51.4)	59.5 (38.7)	69.1 (53.1)	95.9 (93.6)
R_{cryst} (%)	18.5	20.9	19.9	21.2	20.9	21.6
R_{free} (%)	20.7	23.6	23.8	25.2	24.4	26.1
R.m.s. deviations						
Bonds (Å)	0.007	0.007	0.008	0.008	0.008	0.008
Angles (°)	1.46	1.28	1.61	1.31	1.33	1.57
Ramachradran plot						
Most favorable (%)	91.4	90.3	88.2	84.7	87.7	88.5
Additionally allowed (%)	8.6	9.7	11.8	15.3	12.3	11.5
Disallowed (%)	0.0	0.0	0.0	0.0	0.0	0.0
Average *B* factor (Å^2)	36.5	42.0	45.4	48.0	52.5	65.0

† Subunit and residue number shown in parentheses of strain name; the mutation is listed on the second line. ‡ All diffraction data are from crystals in the trigonal space group $P3_121$ (Table 1). § The lower resolution limit was set to 30 Å for all data sets.

some changes to the contact region, but interactions involving the bridging solvent network remain. When Thr*M*21 is replaced by Asp in the TD(*M*21) mutant, most of the electron density for the solvent is lost. Although identification of the molecule bridging *M*21 and *L*71 in the wild type is not definitive, it is most likely a negative ion that is lost owing to an unfavorable interaction with the negatively charged carboxylic group introduced in the TD(*M*21) mutant.

Although residue Glu*L*205 is not directly involved in any contact interaction in the trigonal form, this residue does interact with His*H*68, which is part of a loop that closely interacts with the same region from a symmetry-related protein (Fig. 4). The electron density of the EL(*L*205) mutant indicates that the replacement of Glu by Leu results in the incorporation of an ion near *L*205 and *H*68. Associated with these structural changes is an alteration in the position of *H*68 and a shift of the *H*68–*H*72 loop coupled with the loss of water molecules at the interface between neighboring proteins. Thus, EL(*L*205) mutations led to the loss of specific protein–protein interactions at the contact sites for the trigonal form. Thus, for both the TD(*M*21) and EL(*L*205) mutants there is a specific interaction loss at a contact site for the trigonal form. In both cases, a change in a charged surface residue disrupts an interaction mediated by solvent molecules. The loss of the interacting bridge appears to lead to a significant decrease in the contact strength and a consequent increase in the disorder of the crystal.

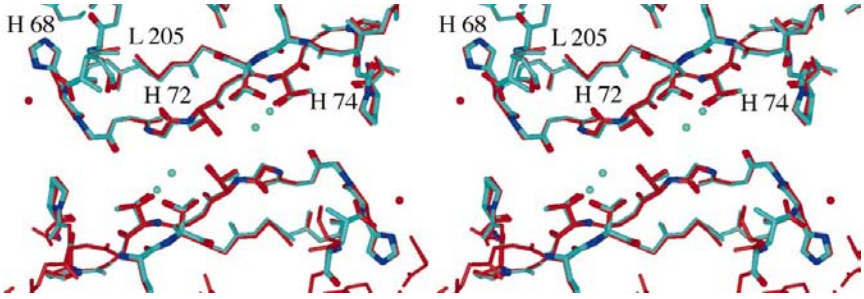

Figure 4
Stereo diagram of a contact region for the trigonal form in the wild type (blue) and the EL(*L*205) mutant (red). In the wild type, Glu*L*205 interacts with His*H*68, which is part of a loop formed by residues *H*68–*H*74 that is close to the same loop of a symmetry-related protein. This contact interaction is mediated by water molecules (blue) associated with Thr*H*72 and Thr*H*74. The substitution of Leu for Glu at *L*205 results in the association of a molecule, probably an ion (red), near *L*205 and *H*68 and loss of the bridging water molecules.

4. Discussion

The nature of the protein–protein contacts was found to have a significant impact on the morphology and diffraction quality of the crystals. The alterations resulted both in the loss of the tetragonal crystals and in changes in the order of the diffraction data for crystals in the trigonal form. The change of a single amino-acid side chain was sufficient to affect the crystal quality, even though the reaction center is large, with over 800 amino acids. Since the structures of the mutants are essentially the same as the wild type, the changes in crystal quality can be interpreted in terms of changes in bond interactions arising from the mutations and not gross structural rearrangements of the backbone. Interactions mediated by ions or water molecules appear to be particularly susceptible to alterations involving ionizable residues because of compensation for changes in the charge distribution on the surface of the protein by the loss or addition of bound solvent molecules.

For water-soluble proteins, the impact of surface residues in controlling protein solubility and providing protein–protein contacts has been established by studies that systematically altered such residues (McElroy *et al.*, 1992; Jenkins *et al.*, 1995; Matthews, 1995; D'Arcy *et al.*, 1999, Longenecker *et al.*, 2001). Single-site mutations were shown to lead to new crystalline forms (see, for example, Longenecker *et al.*, 2001), consistent with the observations for the reaction-center mutants. The applicability of altering surface residues for integral membrane proteins was demonstrated by crystallization studies of two β-barrel proteins, OmpA and OmpX, in which membrane-exposed regions of the protein were mutated (Pautsch *et al.*, 1999).

For both proteins, mutations resulted in new crystalline forms that diffracted better than the native forms. Our results show that mutations of α-helical integral membrane proteins also can produce new forms, indicating that this is probably a general aspect of membrane-protein crystallization.

The role of protein–protein interactions is balanced by the role played by detergent molecules, which occupy a large fraction of the space in crystals of membrane proteins. Since crystals are often formed in conditions near consolute boundaries (Garavito *et al.*, 1996), interactions involving detergent molecules probably help to form protein aggregates. The arrangement of the bulk of the detergent molecules is random, so these interactions necessarily are limited in their ability to order the protein in the crystals. Interactions involving protein side chains and ions provide the specific connections that are needed to precisely arrange the proteins. If the contact interactions are too limited, crystals may form but be too disordered to diffract X-rays to high resolution.

Thus, there are several factors that can be altered in order to improve on the tenuous nature of the contacts needed for the crystallization of membrane proteins. Most crystallization attempts involve changing the composition of crystallization solutions using a trial-and-error process. Complicating the crystallization screening of membrane proteins are the added parameters introduced by the presence of the detergents and amphiphiles. By utilizing conditions that are specific to the choice of detergent, the number of initial conditions tested can be greatly decreased (Garavito *et al.*, 1996). The number of amphiphiles tested in the screening process can be reduced by matching the amphiphiles to physical properties of the detergents (Rosenow *et al.*, 2001). In addition to issues concerning protein solubility and stability, the choice of detergent is crucial, as the detergent molecules can play critical roles in establishing contact sites involving hydrophobic regions of the protein as found in fumarate reductase (Iverson *et al.*, 1999). The use of mutants with alterations of surface-exposed loops can potentially provide new interactions between proteins that will facilitate crystallization. Finally, once crystals are obtained, improvement in the crystalline quality should be achievable by using low-resolution structural models to target the alteration of amino-acid residues that are providing the specific protein–protein interactions at the contact sites.

We wish to thank M. Rosenow for assistance with data collection. Part of this work was performed at the rotation-camera facility at SSRL supported by the DOE and NIH. This research was supported by grant NAG8-1353 from the Microgravity Division of NASA.

References

Allen, J. P. (1994). *Proteins Struct. Funct. Genet.* **20**, 283–286.
Allen, J. P., Feher, G., Yeates, T. O., Komiya, H. & Rees, D. C. (1987). *Proc. Natl Acad. Sci. USA*, **84**, 5730–5734.
Bowie, J. U. (2000). *Curr. Opin. Struct. Biol.* **10**, 435–437.
Brünger, A. T. & Rice, L. M. (1997). *Methods Enzymol.* **277**, 243–269.
Chang, C. H., El-Kabbani, O., Tiede, D., Norris, J. & Schiffer, M. (1991). *Biochemistry*, **30**, 5352–5360.
Chang, G., Spencer, R. H., Lee, A. T., Barclay, M. T. & Rees, D. C. (1998). *Science*, **282**, 2220–2226.
D'Arcy, A., Stihle, M., Kostrewa, D. & Dale, G. (1999). *Acta Cryst.* D**55,** 1623–1625.
Deisenhofer, J., Epp, O., Miki, R., Huber, R. & Michel, H. (1985). *Nature (London)*, **318**, 618–624.
Doyle, D. A., Cabral, J. M., Pfuetzner, R. A., Kuo, A. L., Gulbis, J. M., Cohen, S. L., Chait, B. T. & MacKinnon, R. (1998). *Science*, **280**, 69–77.
Ermler, U., Fritzsch, G., Buchanan, S. K. & Michel, H. (1994) *Structure*, **2**, 925–936.
Feher, G., Allen, J. P., Okamura, M. Y. & Rees, D. C. (1988). *Nature (London)*, **339**, 111–116.
Garavito, R. M., Picot, D. & Loll, P. J. (1996). *J. Bioenerg. Biomembr.* **28**, 13–27.
Iverson, T. M., Luna-Chavez, C., Cecchini, G. & Rees, D. C. (1999). *Science*, **284**, 1961–1966.
Iwata, S., Ostermeier, C., Ludwig, B. & Michel, H. (1995). *Nature (London)*, **376**, 660–669.
Iyer, G. H., Dasgupta, S. & Bell, J. A. (2000). *J. Cryst. Growth*, **217**, 429–440.
Jenkins, T. M., Hickman, A. B., Dyda, F., Ghirlando, R., Davies, D. R. & Craigie, R. (1995). *Proc. Natl Acad. Sci. USA*, **92**, 6057–6061.
Jones, T. A., Zou, J. Y., Cowan, S. W. & Kjeldgaard, M. (1991). *Acta Cryst.* A**47**, 110–119.
Koepke, J., Hu, X., Muenke, C., Schulten, K. & Michel, H. (1996). *Structure*, **4**, 581–589.
Laskowski, R. A., MacArthur, M. W., Moss, D. S. & Thornton, J. M. (1993). *J. Appl. Cryst.* **26**, 283–291.
Leslie, A. G. W. (1999). *Acta Cryst.* D**55**, 1696–1702.
Longenecker, K. L., Garrard, S. M., Sheffield, P. J. & Derewenda, Z. S. (2001). *Acta Cryst.* D**57**, 679–688.
McAuley, K. E., Fyfe, P. K., Ridge, J. P., Isaacs, N. W., Cogdell, R. J. & Jones, M. R. (1999). *Proc. Natl Acad. Sci. USA*, **96**, 14706–14711.
McDermott, G., Prince, S. M., Freer, A. A., Hawthornthwaite-Lawless, A. M., Papiz, M. Z., Cogdell, R. J. & Isaacs, N. W. (1995). *Nature (London)*, **374**, 517–521.
McElroy, H. E., Sisson, G. W., Schoettlin, W. E., Aust, R. M. & Villafranca, J. E. (1992). *J. Cryst. Growth*, **122**, 265–272.
McRee, D. E. (1993). *Practical Protein Crystallography*. New York: Academic Press.
Matthews, B. W. (1995). *Adv. Protein Chem.* **46**, 249–278.
Merritt, E. A. & Bacon, D. J. (1997). *Methods Enzymol.* **277**, 505–524.
Otwinowski, Z. & Minor, W. (1997). *Methods Enzymol.* **276**, 307–326.
Pautsch, A., Vogt, J., Model, K., Siebold, C. & Schulz, G. E. (1999). *Proteins Struct. Funct. Genet.* **34**, 167–172.
Rosenow, M. A., Williams, J. C. & Allen, J. P. (2001). *Acta Cryst.* D**57**, 925–927.
Stowell, M. H. B., McPhillips, T. M., Rees, D. C., Soltis, S. M., Abresch, E. & Feher, G. (1997). *Science*, **276**, 812–816.
Tsukihara, T., Aoyama, H., Yamashita, E., Tomizaki, T., Yamaguchi, H., Shinzawa-Itoh, K., Nakashima, R., Yaono, R. & Yoshikawa, S. (1996). *Science*, **272**, 1136–1144.
Williams, J. C., Alden, R. G., Murchison, H. A., Peloquin, J. M., Woodbury, N. W. & Allen, J. P. (1992). *Biochemistry*, **31**, 11029–11037.
Xia, D., Yu, C.-A., Kim, H., Xia, J.-Z., Kachurin, A. M., Zhang, L., Yu, L. & Deisenhofer, J. (1997). *Science*, **277**, 60–66.
Zhang, Z., Huang, L. S., Schulmeister, V. M., Chi, Y.-I., Kim, K. K., Hung, L.-W., Crofts, A. R., Berry, E. A. & Kim, S.-H. (1998). *Nature (London)*, **392**, 677–684.